Available online at www.sciencedirect.com
SCIENCE DIRECT®

Polymer 44 (2003) 5691–5699

polymer

www.elsevier.com/locate/polymer

Plane stress fracture toughness of physically aged plasticized PETG as assessed by the essential work of fracture (EWF) method

J. Karger-Kocsis[a,*], T. Bárány[b], E.J. Moskala[c]

[a]Institut für Verbundwerkstoffe GmbH, Technische Universität Kaiserslautern, P.O. Box 3049, D-67653 Kaiserslautern, Germany
[b]Department of Polymer Engineering and Textile Technology, Faculty of Mechanical Engineering, Budapest University of Technology and Economics, H-1111 Budapest, Hungary
[c]Eastman Chemical Co., Research Laboratories, Kingsport, TN 37662-5150, USA

Received 5 February 2003; received in revised form 27 June 2003; accepted 30 June 2003

Abstract

The plane stress fracture toughness of amorphous copolyester (PETG) sheets plasticized by various amount of neopentylglycol dibenzoate (NPGDB in 0, 5, 10 and 20 wt%) was studied in as-received (AR) and rejuvenated (RJ) states by adopting the essential work of fracture (EWF) method. EWF tests were performed on deeply double-edge notched tensile loaded (DDEN-T) specimens at various deformation rates (2,10 and 100 mm/min) at room temperature. It was established that physical aging strongly affected the EWF terms. The specific yielding-related EWF increased with increasing deformation rate and decreased with increasing plasticizer content. The specific non-essential work and its necking-related constituent, which changed parallel to each other, remained constant up to 10 wt% NPGDB content and decreased afterwards. The plastic zone in the DDEN-T specimens was formed by cold drawing which is governed by the entanglement structure. This was demonstrated by the shape recovery of the plastic zone in the broken DDEN-T specimens after heating them above the T_g of the related PETG compound.

Keywords: Amorphous copolyester; Plasticizer; Essential work of fracture (EWF)

1. Introduction

Recently, the essential work of fracture (EWF) approach has gained acceptance for assessing the toughness of ductile polymers, especially in their sheet form (plane stress conditions prevails). It was shown earlier that amorphous copolyesters are likely the best model materials for the EWF approach as all prerequisites of the method are met [1–3]. The EWF response of amorphous (co)polyesters was already studied as a function of testing conditions (e.g. specimen thickness [4], strain rate [5,6], notching methodology [7], temperature [8]), molecular composition [9] and molecular weight [10]. On the other hand, less information is available on the effects of physical aging and plasticization. The physical aging of thermoplastic (co)polyesters was addressed only by Liu and Nairn [11] and by us [3]. This is quite surprising considering the fact that the mechanical performance of glassy polymers strongly changes with progressing aging. Note that the effect of aging associated generally with severe embrittlement that can be 'erased' by heating the material beyond its glass transition (T_g) and keeping there for a few minutes (rejuvenation procedure). The 'age' of the copolyester is usually estimated by considering the increase in the yield strength if the related function (i.e. yield strength vs aging time under isothermal conditions) is known.

The effect of plasticization on mechanical properties is also of great importance. Of particular interest is the phenomenon known as antiplasticization, which may occur at low plasticizer loadings. Antiplasticization results in an increase in stiffness and yield strength despite the reduced T_g of the plasticizer/polymer mixture [12]. At higher loadings, the plasticizer serves to reduce stiffness and T_g concurrently.

The goal of this study was to determine the effects of strain rate, physical aging and plasticizer content on the EWF response of an amorphous copolyester.

* Corresponding author. Tel.: +49-631-2017203; fax: +49-63-120-171-98.

E-mail address: karger@ivw.uni-kl.de (J. Karger-Kocsis).

0032-3861/03/$ - see front matter © 2003 Elsevier Ltd. All rights reserved.
doi:10.1016/S0032-3861(03)00590-1

2. EWF method

The EWF theory, credited to Broberg ([1–3,13] and references therein) splits the total energy required to fracture a precracked specimen in two components: the essential (W_e) and non-essential work (W_p) of fracture, respectively. W_e is needed to fracture the polymer in the process zone and thus generate new surfaces. W_p is the actual work consumed in the outer plastic region where various energy dissipation mechanism take place. The total fracture energy, W_f, calculated from the area of the force-elongation curves, can thus be expressed by (cf. Fig. 1(a)):

$$W_f = W_e + W_p \tag{1}$$

Considering the surface- (i.e. Lt) and volume-dependence (i.e. L^2t) of the constituent terms, Eq. (1) can be rewritten into the specific terms:

$$W_f = w_e Lt + \beta w_p L^2 t \tag{2}$$

$$w_f = \frac{W_f}{Lt} = w_e + \beta w_p L \tag{3}$$

where L is the ligament length, t is the specimen thickness and β is a shape factor related to the form of the plastic zone. The basic prerequisite of the EWF method is that the ligament (L) of the specimen should be fully yielded before the crack propagation starts. Based on Eq. (3), w_e can be estimated from the interception of the linear regression of the plot of w_f vs L with the w_f-axis. w_e or more exactly the critical value of w_e under mode I plane strain conditions ($w_{e,I}$) should represent a material parameter. On the other hand, the slope (βw_p) of the w_f vs L resistance curves, or more exactly w_p, is a direct measure of the resistance to crack growth.

It was found that w_e is a composite term under plane-stress conditions consisting of yielding ($w_{e,y}$) and necking + tearing ($w_{e,n}$) components. The force-elongation behavior displayed in Fig. 1(a) allowed us to partition between the specific work of fracture required for yielding (w_y) and that consumed by necking + tearing (w_n). As a consequence the data reduction given by Eq. 3 is changing for ([1–3,14] and references therein):

$$w_f = w_{f,y} + w_{f,n} = w_e + \beta w_p L \tag{4}$$

$$w_{f,y} = w_{e,y} + \beta' w_{p,y} L \tag{5}$$

$$w_{f,n} = w_{e,n} + \beta'' w_{p,n} L \tag{6}$$

So, the specific EWF (w_e) is a combined term under plane-stress conditions:

$$w_e = w_{e,y} + w_{e,n} \tag{7}$$

This energy partitioning has been proved experimentally for many ductile polymer sheets ([1–3] and references therein).

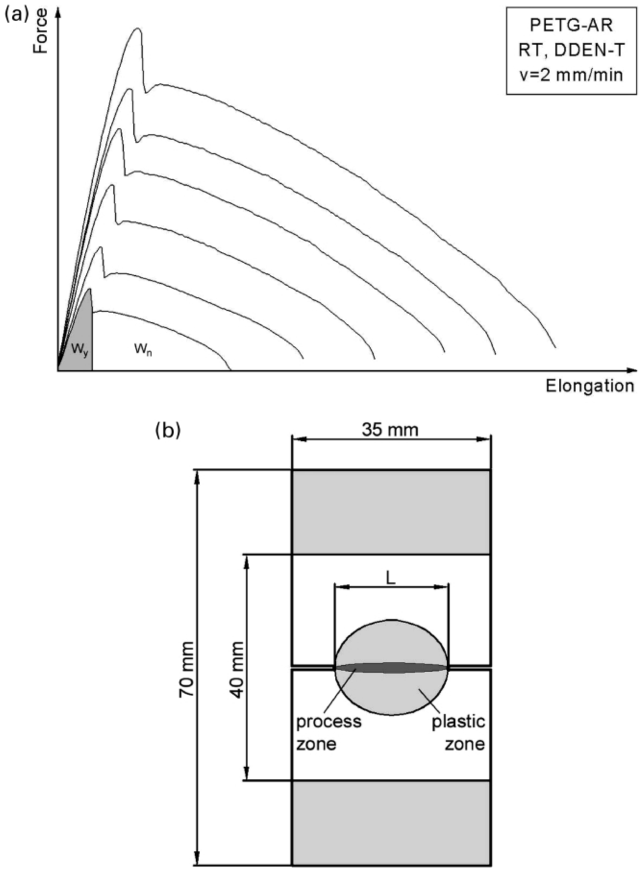

Fig. 1. (a) Characteristic force-elongation curves showing the energy partitioning. (b) Dimension of the DDEN-T specimens.

3. Experimental

3.1. Materials

Plasticized copolyester sheets were produced by compounding Eastar PETG 6763 from Eastman Chemical Company (Kingsport, TN, USA) with neopentylglycol dibenzoate (NPGDB) in a twin-screw extruder ($T = 220–240$ °C, 90 rpm) followed by chill roll ($T = 65$ °C) sheeting. The NPGDB content was varied between 0 and 20 wt%. According to gel permeation chromatography results, the number-average (M_n) and weight-average (M_w) molecular weights were found in the range $(1.1–1.4) \times 10^4$ and $(3.5–3.9) \times 10^4$ g/mol, respectively. T_g values of the compounds with 0, 5, 10 and 20 wt% NPGDB were 77, 60, 49 and 36 °C, respectively. Sheets with a thickness of approximately 0.3 mm were studied both in as-received (AR) and rejuvenated (RJ) stages. AR corresponds to a storage time of about 2 years at ambient temperature and 50% relative humidity. Rejuvenation of the sheets was performed in a thermostatic oven 10 °C above the T_g of the related compound for 15 min. In order to keep the sheet form, the sheets were sandwiched between two preheated glass plates (of ca. 4 mm thickness each).

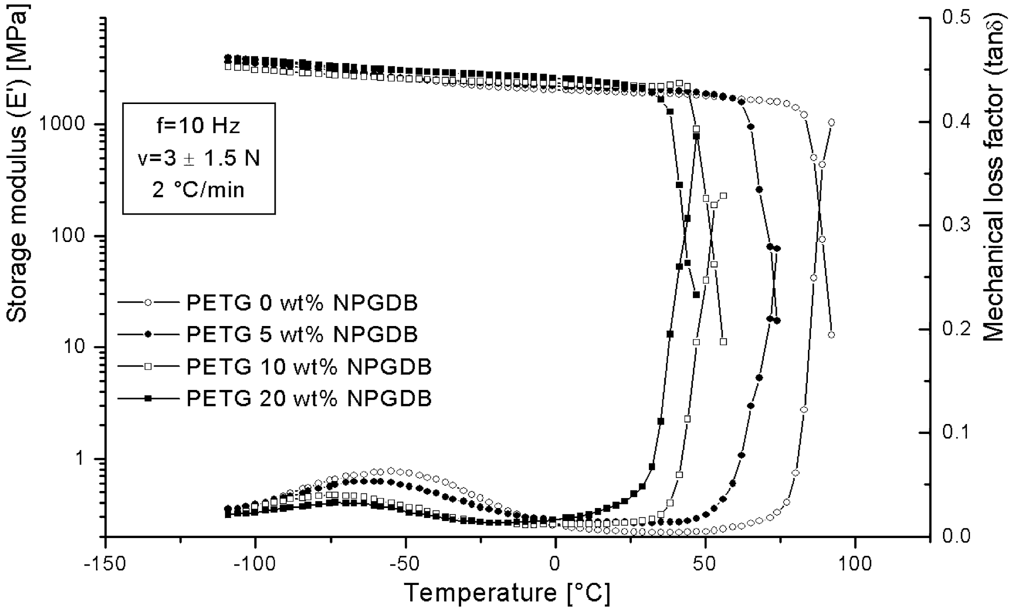

Fig. 2. Change in the storage modulus (E') and mechanical loss factor (tan δ) as a function of temperature for the antiplasticized PETG.

3.2. Material characterization

Dynamic mechanical thermal analysis (DMTA) was performed on rectangular specimens in tensile mode on an Eplexor Quaimeter 25N (Gabo, Ahlden, Germany) using a frequency of 10 Hz and a heating rate of 2 °C/min. The static and oscillating loads were set for 3 and ± 1.5 N, respectively, and the temperature range covered was − 100 to + 100 °C.

Differential scanning calorimetry (DSC) traces were recorded on a Mettler DSC 821 device in the temperature range from − 100 to +300 °C at a heating and cooling rate of 20 °C/min.

3.3. Specimens and their testing

The specimens were oriented along the machine (film production) direction. Static tensile mechanical properties were determined on dumbbells (type 1B according to EN ISO 527) at room temperature (RT) with various deformation rates ($v = 2$, 10 and 100 mm/min). For the EWF study, double deeply edge-notched specimens (DDEN-T) were used by subjecting them to tensile loading at RT at the aforementioned deformation rate. The dimensions of the DDEN-T specimen are given in Fig. 1(b). The free ligament of the DDEN-T specimens ranged from $L = 5$ to 25 mm. The shape factor (β—cf. Eqs. (2)–(4)) was determined by

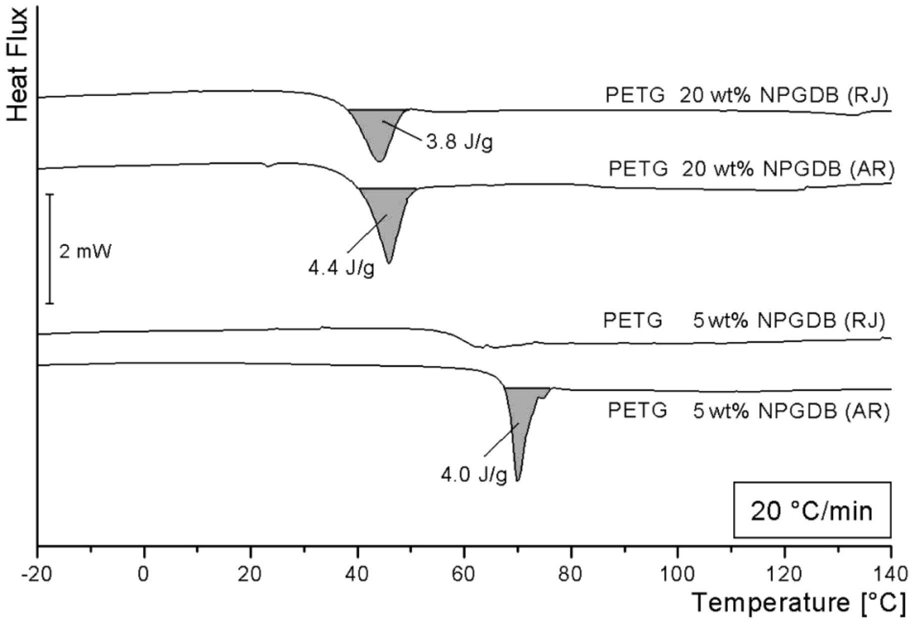

Fig. 3. DSC heating traces taken on the samples containing 5 and 20 wt% antiplasticizer in AR and RJ stages, respectively.

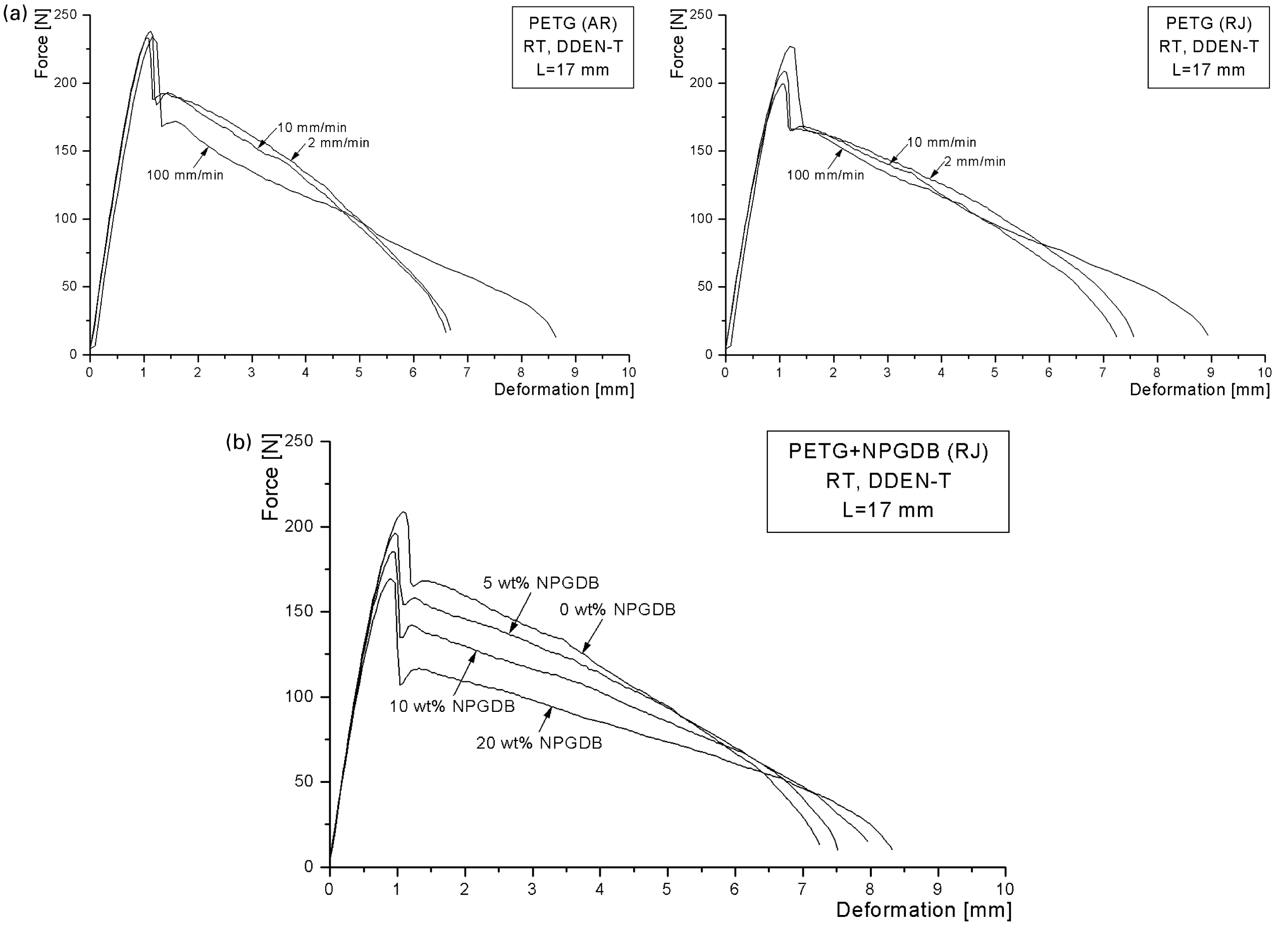

Fig. 4. (a) Force-deformation curves of DDEN-T specimens ($L = 17$ mm) of PETG in AR (left) and RJ stages (right) showing the effect of deformation rate at the same ligament length. (b) Force-deformation curves of DDEN-T specimens ($L = 17$ mm) of PETG in RJ stage showing the effect of antiplasticizer content.

viewing the height of the 'plastic zone' post mortem using a light microscope [4,5,14].

3.4. Fractography

The fracture surface of the DDEN-T specimens was inspected in a scanning electron microscope (Jeol JSM 5400, Japan) after sputtering with a Au/Pd alloy.

4. Results and discussion

4.1. Antiplasticization

Fig. 2 shows the complex storage modulus (E') and mechanical loss factor (tan δ) as a function of temperature for the NPGDB modified PETG in the RJ stage. The plasticization reflected by a continuous decrease in the T_g due to increasing NPGDB is well resolved in the DMTA traces. Further, adding NPGDB to PETG results in slightly enhanced stiffness in the sub T_g region—cf. the E' vs T traces in Fig. 2. At the same time the intensity of the secondary relaxation peak at $T \approx -60$ °C decreases with increasing NPGDB content. These changes are characteristic for a diluent termed antiplasticizer [12].

DSC traces in Fig. 3 demonstrate the difference in the AR and RJ stages for the samples containing 5 and 20 wt% antiplasticizer. As expected, increasing aging is associated with a more prominent enthalpy relaxation peak, which may be a suitable measure of physical aging [11]. Note that enthalpy relaxation is still present after rejuvenation for the sample with 20 wt% plasticizer. This can be traced to the rather small difference between the related T_g and RT where storage and testing occurred. Recall, that the effect of physical aging is the more pronounced the closer the T_g of the polymer to the storage temperature.

4.2. EWF response

Characteristic force-elongation curves of the DDEN-T specimens at comparable ligament length showing the effects of deformation rate, physical aging and plasticizer content are depicted in Fig. 4.

Note that the energy partitioning, shown in Fig. 1(a), could be adopted for all test series where the specimens failed ductilely. This was, however, not always the case—see later. Recall that the specific work of fracture

Table 1
Static tensile mechanical and specific essential work of fracture parameters for the antiplasticized PETG sheets

Material	Stage	Deformation rate (mm/min)	Static tensile (MPa)		Specific essential work (kJ/m^2)		
			E	σ_y	w_e	$w_{e,n}$	$w_{e,y}$
PETG	As received (AR)	2	2230	49.1	51.0	38.0	13.0
		10	2125	53.1	50.7	35.1	15.6
		100[x]	2160	55.8	35.6	17.9	17.7
	Rejuvenated (RJ)	2	1885	41.3	36.1	25.1	10.9
		10	1870	44.7	35.5	23.6	11.9
		100	1955	48.9	30.9	14.4	16.1
PETG + 5 wt% NPGDB	As received (AR)	2	2390	49.6	31.6	17.2	14.4
		10	–	–	Brittle		
		100	–	–	Brittle		
	Rejuvenated (RJ)	2	2085	43.6	35.5	24.3	11.1
		10	2120	48.1	36.8	25.0	11.8
		100[x]	2160	54.5	19.9	8.4	11.4
PETG + 10 wt% NPGDB	As received (AR)	2	–	–	Brittle		
		10	–	–	Brittle		
		100	–	–	Brittle		
	Rejuvenated (RJ)	2	2245	43.0	34.8	24.7	10.1
		10	2270	48.7	34.5	22.0	12.5
		100	2470	58.0	Brittle		
PETG + 20 wt% NPGDB	As received (AR)	2	1370	23.1	36.1	29.2	6.9
		10	1730	33.0	37.3	26.7	10.4
		100	–	–	Brittle		
	Rejuvenated (RJ)	2	1665	29.8	30.3	23.2	6.5
		10	1870	35.3	30.8	21.0	9.7
		100	2145	46.6	Brittle		

[x] the maximum ligament threshold was reduced owing to the onset of brittle fracture.

parameters were determined according to Eqs. (4)–(6) by a linear fitting of the corresponding work of fracture as a function of ligament. As will be disclosed later, the related correlation coefficient (R^2) was always higher than 0.90. Table 1 lists the specific EWF (w_e) and its constituents ($w_{e,y}$ and $w_{e,n}$) as a function of both deformation rate and aging for the plasticized PETG. Table 1 also contains the static mechanical data, viz. E modulus (E) and yield strength (σ_y), measured on dumbbells. Attention should be paid to the fact that both E and σ_y of the plasticized sheets fairly agree with those of the unmodified PETG at least up to 10 wt% NPGDB content (cf. RJ data in Table 1). This is a clear indication of the antiplastication due to NPGDB. One can see that rejuvenation and deformation rate usually cause a decrease in w_e. However, it is more straightforward to focus on the yielding related specific EWF, $w_{e,y}$. Recall that this term is considered as a material parameter

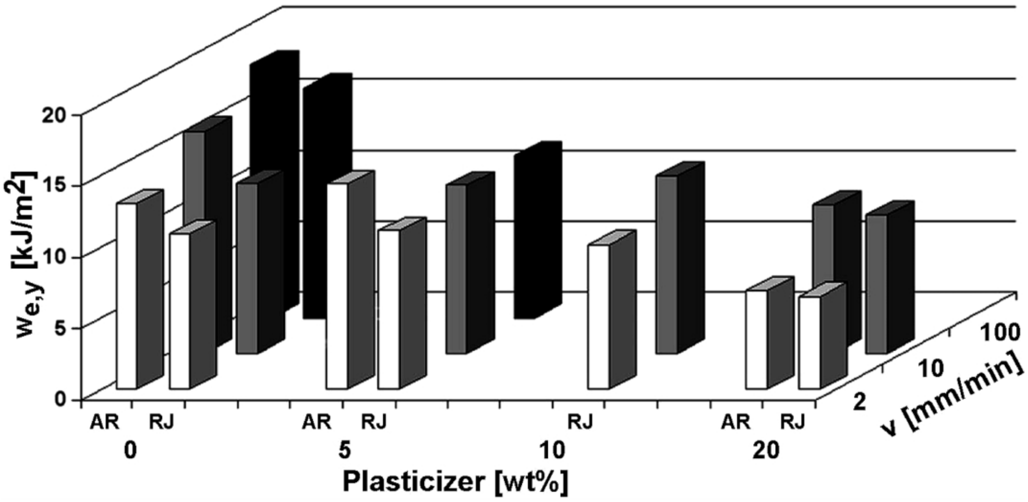

Fig. 5. Change in $w_{e,y}$ as a function of aging, deformation rate and antiplasticizer content.

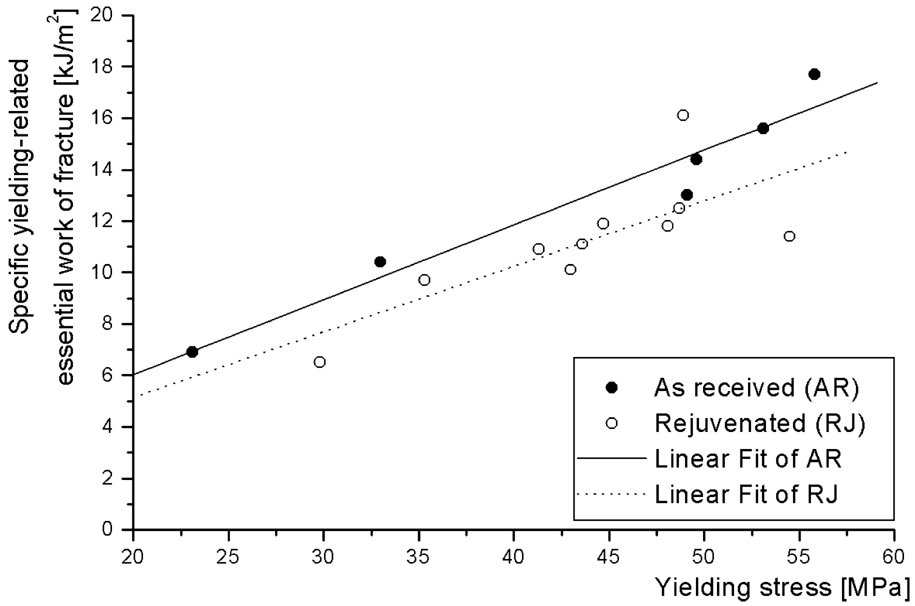

Fig. 6. $w_{e,y}$ and σ_y plot for the antiplasticized PETG sheets investigated.

which represents the inherent toughness [1–4,15]. Fig. 5 shows that $w_{e,y}$ increases with increasing deformation rate and decreases with increasing plasticizer content. The latter substantiates the plasticizing effect of NPGDB.

Table 1 contains a further very useful relationship. Plotting the corresponding $w_{e,y}$ against σ_y a fair linear correlation can be deduced—cf. Fig. 6. The correlation in Fig. 6 suggests a relationship between the static tensile and EWF responses. As a consequence, the effect of aging can be traced by $w_{e,y}$ in addition to σ_y (which is the present praxis) [3].

Table 2
Specific non-essential work of fracture parameters for the antiplasticized PETG sheets

Material	Stage	Deformation rate (mm/min)	Specific non-essential work of fracture (MJ/m^3)						
			Eq. 4			Eq. 5		Eq. 6	
			βw_p	R^2	β^*	$\beta' w_{p,y}$	R^2	$\beta' w_{p,n}$	R^2
PETG	As received (AR)	2	6.6	0.98	0.061	1.1	0.98	5.5	0.98
		10	6.6	0.98	0.056	1.1	0.90	5.5	0.98
		100^x	8.5	0.99	0.076	1.2	0.93	7.3	0.98
	Rejuvenated (RJ)	2	7.5	0.99	0.067	1.3	0.99	6.4	0.99
		10	7.5	0.99	0.065	1.3	0.98	6.2	0.99
		100	8.7	0.99	0.083	1.5	0.98	7.2	0.99
PETG + 5 wt% NPGDB	As received (AR)	2	7.5	0.94	0.061	1.1	0.96	6.3	0.93
		10	Brittle						
		100	Brittle						
	Rejuvenated (RJ)	2	7.9	0.99	0.066	1.1	0.97	7.0	0.99
		10	7.5	0.99	0.066	1.0	0.95	6.5	0.99
		100^x	9.6	0.99	0.078	1.3	0.97	8.1	0.99
PETG + 10 wt% NPGDB	As received (AR)	2	Brittle						
		10	Brittle						
		100	Brittle						
	Rejuvenated (RJ)	2	7.5	0.99	0.063	1.0	0.94	6.5	0.99
		10	7.4	0.99	0.074	0.9	0.93	6.5	0.99
		100	Brittle						
PETG + 20 wt% NPGDB	As received (AR)	2	6.3	0.99	0.071	1.3	0.98	5.0	0.99
		10	6.2	0.99	0.086	1.1	0.97	5.0	0.99
		100	Brittle						
	Rejuvenated (RJ)	2	6.4	0.99	0.065	1.2	0.97	5.2	0.99
		10	6.4	0.99	0.071	1.0	0.97	5.3	0.99
		100	brittle						

β^* is dimensionless; ^{x} at a given deformation rate means that the maximum threshold ligament was reduced owing to brittle fracture.

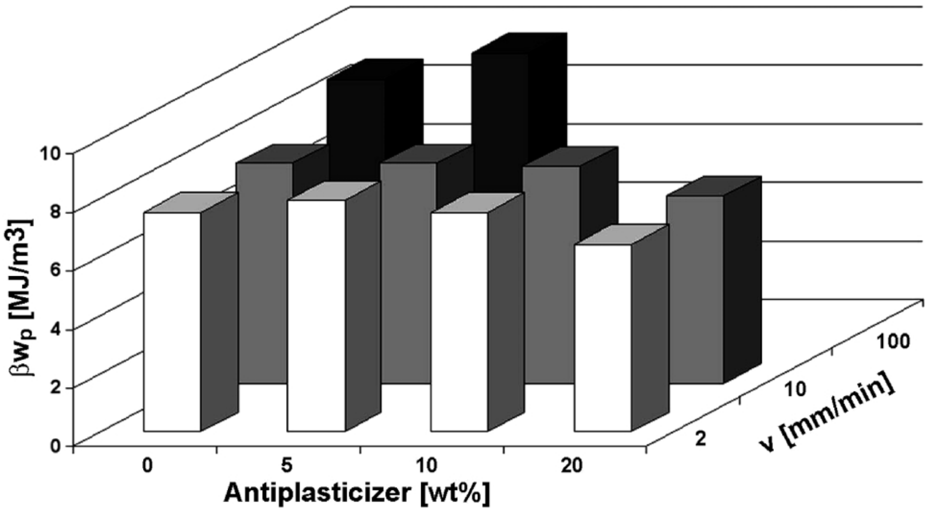

Fig. 7. Change in βw_p as a function of deformation rate and antiplasticizer content for the rejuvenated sheets.

Table 2 lists the non-EWF terms—cf. Eqs. (4)–(6). Note that this table contains also the correlation coefficients of the linear regressions according to the above Equations. The shape parameter β was determined by the method used in Refs. [4,5,14] assuming a diamond shape plastic zone (cf. later). βw_p, i.e. the slope of the linear regression according to Eq. 4, is constant at a deformation rate ≤ 10 mm/min for all samples. At higher deformation rate βw_p increased (if the specimens did not undergo brittle fracture). A similar trend holds also for $\beta'' w_{p,n}$ as $\beta' w_{p,y}$ is less affected by the deformation rate. The most striking effect of the plasticizer content is that both βw_p and $\beta'' w_{p,n}$ remain practically unaffected up to 10 wt% NPGDB before they became slightly reduced at higher NPGDB content—cf. Fig. 7. The shape parameter β, which marginally increased with the deformation rate, was nearly unaffected by the plasticizer content. Accordingly, the necking + tearing behavior does not depend much on the plasticizer content, at least for the RJ stage and up to 10 wt% NPGDB. It is worth noting that RJ increased both βw_p and $\beta'' w_{p,n}$ terms for all systems except for PETG with the highest NPGDB content. For this compound, no difference was found between the AR and RJ stages. This is in harmony with the DSC (cf. Fig. 2) and tensile mechanical results (cf. Table 1) and can be attributed to the 'fast' aging of this compound having slightly higher T_g (36 °C) than RT.

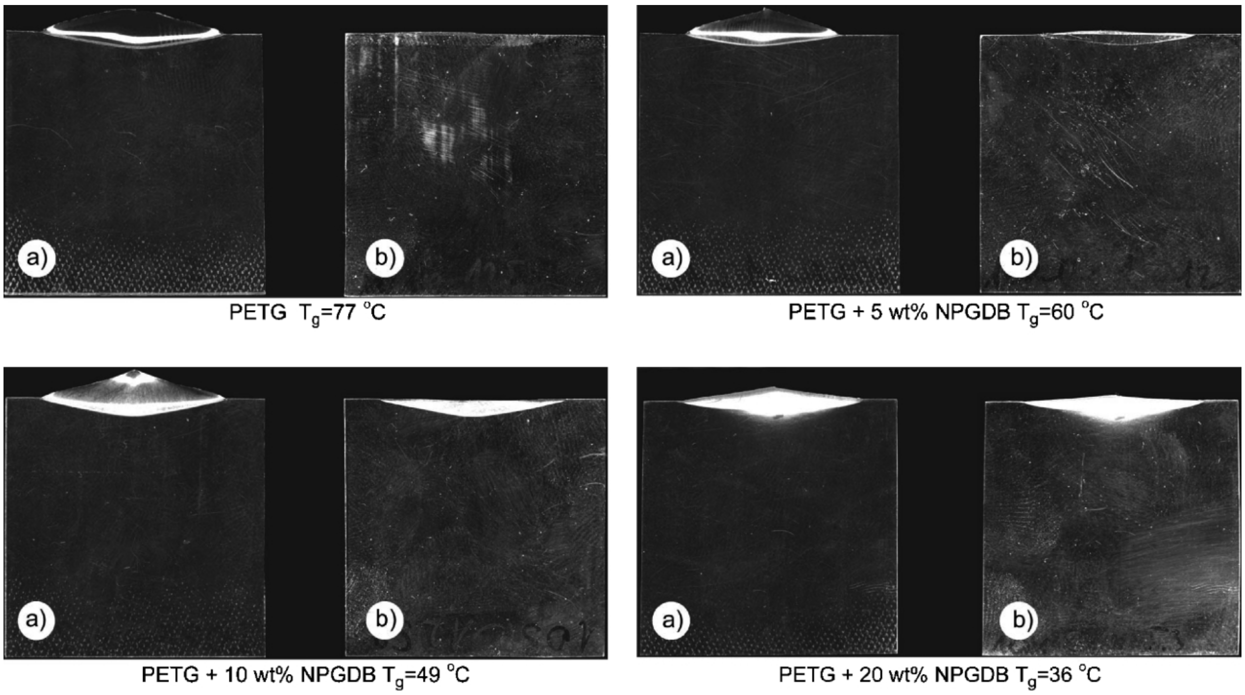

Fig. 8. Restoration of the plastic zone by annealing above the T_g. Designations: broken half of the DDEN-T specimen before (a) and after annealing (b).

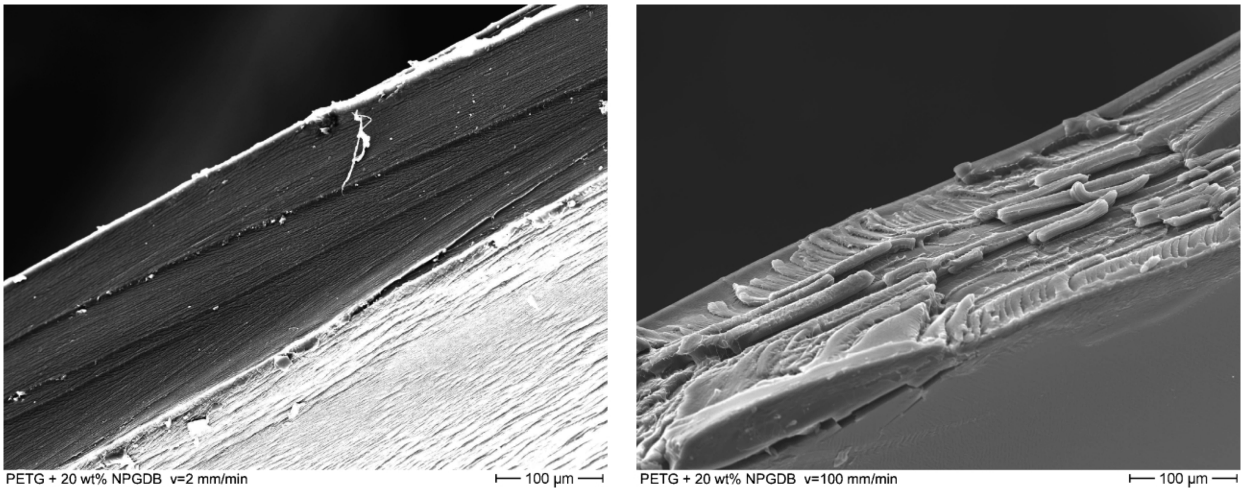

Fig. 9. SEM picture taken on the fracture surface of the DDEN-T specimens of PETG with 20 wt% NPGDB content with deformation rate of 2 (left) and 100 mm/min (right).

4.3. Failure

Fig. 8 displays macrophotographs of the ligament area of failed DDEN-T specimens cut with various plasticizer contents before and after annealing just above the related T_g ($T_g + 10\,°C$ *for* 15 min). Note that this condition agrees with that of the rejuvenation. Based on Fig. 8 one can claim that the plastic zone in the DDEN-T specimens was formed by cold drawing, instead of true plastic deformation, as this zone fully recovers (except PETG with 20 wt% NPGDB—cf. Fig. 8). This recovery process is governed by the entanglement network. It was suggested that the entanglement network controls the fracture mechanical response of amorphous polymer glasses [2]. The finding that βw_p and $\beta'' w_{p,n}$ did not change with the plasticizer content (NPGDB content ≤ 10 wt%) suggests that the entanglement characteristics were also not affected. Increasing stress whitening and less complete recovery of the plastic zone can be noticed at high NPGDB content (cf. pictures b) of the samples with 10 and 20 wt% NPGDB in Fig. 8). This suggests that cold drawing might have been accompanied with strain-induced crystallization. This aspect, documented for amorphous polyethylene terephthalate [16], will be evaluated in future studies.

It has been already demonstrated in Tables 1 and 2 that aged specimens subjected to increasing deformation rates failed in a brittle manner (cf. Fig. 9). A ductile/brittle transition was also observed to occur as a function of the ligament length under the same experimental conditions. In such cases, the 'valid' ligament range was reduced before determining the specific work of fracture terms.

5. Conclusions

Based on this work devoted to assessing the plane stress fracture toughness of PETG sheets plasticized by neopentylglycol dibenzoate (NPGDB) in physically aged (as received, AR) and rejuvenated (RJ) stages using the EWF method, the following conclusions can be drawn.

- Progressive physical aging can be followed by the increase in the yielding-related specific EWF term. This term correlates well with the yield strength, which is widely used to trace the aging.
- The specific yielding-related EWF increased with increasing deformation rate (from 2 to 100 mm/min) and decreased with increasing NPGDB content (from 0 to 20 wt%).
- The specific non-EWF and its necking-related constituent changed parallel to each other. They were fairly constant for the compounds at each deformation rate up to 10 wt% NPGDB and decreased above this threshold.
- The plastic zone in the specimens was formed by cold drawing as it was recovered by heating the broken specimens above the T_g of the related compound. The onset of stress whitening and a less complete recovery of the plastic zone at high NPGDB content may be attributed to strain-induced crystallization phenomena.

References

[1] Karger-Kocsis J. In: Williams JG, Pavan A, editors. Fracture of polymers, composites and adhesives, 27. Oxford: Elsevier Science; 2000. p. 213.
[2] Karger-Kocsis J. In: Fakirov S, editor. Handbook of thermoplastic polyesters, vol. 1. Wiley-VCH: Weinheim; 2002. p. 717.
[3] Karger-Kocsis J, Moskala EJ. SPE-ANTEC 2002;60:1751.
[4] Karger-Kocsis J, Czigány T, Moskala EJ. Polymer 1997;38:4587.
[5] Karger-Kocsis J, Czigány T, Moskala EJ. Polymer 1998;39:3939.
[6] Ching ECY, Li RKY, Mai Y-W. Polym Engng Sci 2000;40:310.
[7] Poon WKY, Ching ECY, Cheng CY, Li RKY. Polym Test 2001;20: 395.
[8] Arkhireyeva A, Hashemi S. J Mater Sci 2002;37:3675.

[9] Mouzakis DE, Karger-Kocsis J, Moskala EJ. J Mater Sci Lett 2000; 19:1615.
[10] Karger-Kocsis J, Moskala EJ. Polym Bull 1997;39:503.
[11] Liu C-H, Nairn JA. Polym Engng Sci 1998;38:186.
[12] Chartoff RP. In: Turi EA,, editors, 2nd ed. Thermal characterization of polymeric materials, vol. 1. New York: Academic Press; 1981. p. 662.
[13] Mai Y-W, Wong S-C, Chen X-H. In: Paul DR, Bucknall CB, editors. Polymer blends formulations and performance, vol. 2. New York: Wiley; 1999. p. 17.
[14] Karger-Kocsis J, Moskala EJ. Polymer 2000;41:6301.
[15] Karger-Kocsis J, Ferrer-Balas D. Polym Bull 2001;46:507.
[16] Karger-Kocsis J, Moskala EJ, Shang PP. J Therm Anal Calorim 2001; 63:671.